THE ASTROPHYSICAL JOURNAL, **208**:753–759, 1976 September 15

THE 10 MICRON SILICATE FEATURE IN SOUTHERN H II REGIONS

S. ERIC PERSSON,*† JAY A. FROGEL,*‡§ AND MARC AARONSON*§
Received 1975 September 29; revised 1976 January 16

ABSTRACT

Intermediate-band photometric measurements in the 10 μ region are presented for 22 infrared sources associated with southern H II regions. The energy distributions display substantial silicate absorption with optical depths at band center (9.8 μ) ranging from 0.4 to 5.0. The depth of the 9.8 μ band is related to the depth of 6 cm formaldehyde absorption in the sense that $\tau(9.8\ \mu)$ must exceed 2 for $\tau(H_2CO)$ to exceed 0.03. The effect of the silicate absorption is to attentuate the intrinsic 1–25 μ luminosities by as much as a factor of 5.

Subject headings: infrared: general — interstellar: molecules — nebulae: general

I. INTRODUCTION

High-resolution ($\Delta\lambda/\lambda \sim$ 0.01–0.02) spectra in the 8–13 μ region of a number of young galactic objects have revealed a broad spectral feature, which, apart from a scaling factor (optical depth), is similar in all sources. Examples are the Trapezium region of Orion (Stein and Gillett 1969), the BN–KL complex (Gillett and Forrest 1973), W3/IRS 5 (Aitken and Jones 1973), the galactic center (Woolf 1972; Aitken and Jones 1973), G333.6−0.2 (Aitken and Jones 1974), and AFCRL 809–2992 in Cygnus (Merrill and Soifer 1974). These authors have attributed this spectral feature to emission and/or absorption by silicate particles.

This paper presents new intermediate bandwidth data in the 8–13 μ region for 22 southern infrared sources. Compared with spectrophotometry ($\Delta\lambda/\lambda \sim$ 0.01), this type of observation had the advantages of speed and large aperture capability, but the potential disadvantage of missing narrow spectral features such as are seen in planetary nebulae and external galaxies. Available evidence does not indicate that this should be a problem for the type of objects considered in this paper.

The model-fitting procedure of Gillett *et al.* (1975) is applied to our data and gives a satisfactory representation of all the spectra. Source temperatures and 9.8 μ optical depths are derived via the models. The optical depths are then compared with other measures of the line-of-sight absorption to these sources. In particular, the correlation between $\tau(9.8\ \mu)$ and the 6 cm formaldehyde absorption noted by Frogel and Persson (1974) (hereinafter referred to as FP) is examined in more detail.

* Center for Astrophysics, Harvard College Observatory, and Smithsonian Astrophysical Observatory.

† Hale Observatories, Carnegie Institution of Washington, and California Institute of Technology.

‡ Cerro Tololo Inter-American Observatory, which is operated by the Association of Universities for Research in Astronomy, Inc., under contract with the National Science Foundation.

§ Guest Investigator, Las Campanas Observatory, Carnegie Institution of Washington.

II. OBSERVATIONAL RESULTS

The observations were made on the 1 m telescope at Las Campanas Observatory, Chile, in 1974 May and 1975 January and April. The data were obtained with a Ge:Ga bolometer equipped with cooled focal plane apertures and a cooled 8–13 μ filter. The intermediate bandwidth filters were outside the Dewar at the ambient temperature. The central wavelengths and half-power bandwidths of these filters are: 8.8 μ, 1.0 μ; 9.8 μ, 0.9 μ; 10.6 μ, 1.75 μ; 11.7 μ, 2.6 μ; 12.6 μ, 1.2 μ. The observations were made with a conventional infrared photometer and a wobbling secondary mirror. Chopping was in an east-west direction with beam separations between 30″ and 45″, but no corrections were applied to the measurements for flux in the reference beam. Typically, such corrections would increase the 10 μ fluxes by only 10–20 percent since the brightness profiles are sharply peaked. The aperture sizes employed and the observed 10 μ ($\Delta\lambda = 5\ \mu$) fluxes are given in Table 1. The intermediate-band fluxes are given in Table 2 and are plotted in Figure 1 as adjusted for filter response (see below). The broadband energy distributions, maps, and other infrared data for some of these sources are in FP and Becklin *et al.* (1973, 1974). OH 284.2−0.8, a peculiar OH emitter having no apparent radio continuum counterpart, was discussed by Frogel and Persson (1975). Additional infrared data for the new sources will be published elsewhere (Frogel, Persson, and Aaronson 1976). One object reported in FP, RCW 49, is not included in the present paper because of incomplete observations.

The error bars in Figure 1 are 1 σ_m errors. To the purely statistical errors was added a 0.05 mag error, in quadrature, to account for nonstatistical errors in the photometry due to guiding, extinction changes, standards calibration, and centering. Comparison of data taken on different nights shows that this is a reasonable estimate.

The dashed lines in Figure 1 are schematic representations of published high-resolution spectra for three of the sources. For η Car (Aitken and Jones 1973)

TABLE 1

Observed and Derived Parameters for H II Regions

Galactic Source	Other Names	Position Measured† (1950.0)		Log $F_\lambda(10\mu)$ ($W\ cm^{-2}\ \mu^{-1}$)	Aper. (")	$\tau(9.8\mu)$	T(°K)	$\chi^2/(N-3)$	Δ Log $F_\lambda(10\mu)$	$\tau(H_2CO)$	Log $N(H_2CO)$ (cm^{-2})	A_V	$\tau(3.1\mu)$
G268.0-1.1	RCW 38	$08^h57^m24^s.2$	-47°18'50"	-15.18	22	0.4	175	1.1	-0.12	0.06	13.23	11	0.25
G274.0-1.1	RCW 42	09 22 45.5	-51 46 27	-15.98	22	1.8	234	1.5	-0.52	0.01	12.88	15	
G282.0-1.2		10 04 55.9	-56 57 49	-16.11	22	2.7	245	5.6	-0.76	0.01	12.37	15	
OH284.2-0.8		10 19 44.4	-57 50 40	-15.25	15	1.9	237	0.5	-0.55				1.15
G285.3-0.0		10 29 35.7	-57 46 37	-16.03	29	2.5	271	3.2	-0.73	0.01	12.80	5	
G291.3-0.7	RCW 57 NGC 3576	11 09 46.3	-61 02 09	-15.50	15	3.5	222	1.9	-0.94	0.05	13.17	15	0.65
G291.6-0.5	NGC 3603	11 12 51.1	-60 59 38	-15.49	22	1.5	222	1.7	-0.44	0.01	12.08		
G298.2-0.3		12 07 22.5	-62 33 20	-15.25	15	1.5	197	1.8	-0.43	0.01	12.43	14	0.17
G327.3-0.6	RCW 97	15 49 12.9	-54 26 27	-15.66	29	3.1	267	3.7	-0.88	0.14	13.61	20	
G333.1-0.4		16 17 14.6	-50 28 50	-16.23	22	3.7	333	0.4	-1.05	0.10	13.74		
G333.3-0.4		16 17 44.1	-50 18 02	-15.79	22	4.9	257	3.3	-1.28	0.20	13.83		
G333.6-0.2		16 18 22.5	-49 59 00	-14.48	15	2.0	229	0.5	-0.57	0.03	13.14	18	0.25
G336.5-1.5	RCW 108	16 36 14.6	-48 45 53	-15.54	29	2.7	288	1.7	-0.78	0.08	13.49	11	0.35
G337.9-0.5N		16 37 27.1	-47 01 00	-15.96	22	3.1	272	1.3	-0.88	0.10	13.55	12	
G337.9-0.5S		16 37 27.1	-47 01 58	-16.19	22	3.1	233	0.6	-0.86				
G340.8-1.0	RCW 110B	16 50 40.3	-45 12 32	-16.22	29	(4)	-	-	(-1.00)	0.15	13.65	20	
G345.4-0.9	H2-3, RCW 117	17 06 01.5	-41 32 20	-15.45	29	2.4	264	1.9	-0.70	0.04	13.00		0.52
G348.2-1.0	H2-6, RCW 121	17 14 57.3	-39 16 16	-16.03	29	2.3	266	4.4	-0.67				
G348.7-1.0	RCW 122	17 16 39.9	-38 54 15	-15.68	22	3.5	248	0.1	-0.96	0.07	13.33		
G351.6-1.3		17 25 53.0	-36 37 49	-16.04	22	4.6	260	2.3	-1.22	0.13	13.64		
G353.2+0.9	W22 NGC 6357	17 21 24.1	-34 08 24	-15.41	29	2.3	288	3.5	-0.68	0.00	12.08		
G10.2-0.3	W31	18 06 31.1	-20 20 10	-15.79	29	3.1	239	3.6	-0.86	0.12	13.97		
G12.8-0.2	W33	18 11 18.3	-17 57 30	-16.06	*	4.8	252	0.5	-1.25	0.46	14.26		

*15" and 22" aperture measurements combined

†Accurate positions of peak surface brightness will be published later.

TABLE 2

Intermediate-band Observations

Source	Log F_λ (W cm^{-2} μ^{-1})* 8.8 μ	9.8 μ	10.6 μ	11.7 μ	12.6 μ
G268.0-1.1	-15.45	-15.20	-15.10	-15.17	-15.19
G274.0-1.1	-16.11	-16.14	-15.99	-16.00	-15.96
G282.0-1.2	-16.25	-16.37	-16.16	-16.16	-15.97
OH284.2-0.8	-15.38	-15.37	-15.29	-15.27	-15.23
G285.3-0.0	-16.14	-16.11	-16.20	-16.07	-16.01
G291.3-0.7	-15.70	-15.84	-15.80	-15.48	-15.29
G291.6-0.5	-15.64	-15.58	-15.48	-15.51	-15.47
G298.2-0.3	-15.46	-15.37	-15.21	-15.24	-15.18
G327.3-0.6	-15.79	-16.00	-15.79	-15.74	-15.58
G333.1-0.4	-16.24	-16.53	-16.43	-16.26	-16.13
G333.3-0.4	-15.94	-16.37	-16.04	-15.79	-15.52
G333.6-0.2	-14.60	-14.59	-14.52	-14.46	-14.41
G336.5-1.5	-15.60	-15.78	-15.62	-15.60	-15.51
G337.9-0.5N	-16.07	-16.29	-16.10	-16.01	-15.87
G337.9-0.5S	-16.34	-16.50	-16.30	-16.16	-16.01
G340.8-1.0	-16.14	-16.62	...	...	...
G345.4-0.9	-15.50	-15.56	-15.50	-15.46	-15.35
G348.2-1.0	-16.13	-16.25	-16.07	-16.10	-15.98
G348.7-1.0	-15.84	-16.08	-15.87	-15.68	-15.55
G351.6-1.3	-16.11	-16.50	-16.23	-15.98	-15.73
G353.2+0.9	-15.46	-15.47	-15.52	-15.44	-15.40
G10.2-0.3	-15.99	-16.31	-15.90	-15.86	-15.69
G12.8-0.2	-16.27	-16.77	-16.37	-16.04	-15.88
BN	-14.89	-15.21	-15.06	-14.89	-14.67

*1 σ_m errors are typically 0.02-0.04. The cases for which the errors are larger can be found from Figure 1.

the color agreement is good, although the absolute flux levels differ somewhat. This could be due to the extended nature of η Car. For G333.6−0.2 (Aitken and Jones 1974), the color agreement is satisfactory, but the flux levels differ by $\Delta \log F_\lambda = 0.2$. This difference most likely arises from the fact that Aitken and Jones used a smaller aperture (12″) and smaller beam separation (15″) than were used in our measurements (15″ and 45″, respectively). For BN, the agreement with the spectrum of Gillett and Forrest (1973) is satisfactory in view of the complicated structure of the emission and absorption near BN, and the difference in chopper orientation. Recent intermediate-band observations of BN by Gehrz, Hackwell, and Smith (1975) show a similar discrepancy compared with Gillett and Forrest's (1973) spectrum between 9 and 11 μ.

In most cases, the position measured was that of maximum 10 μ surface brightness. Although we do not as yet have such information on changes in the shape of the silicate absorption over the sources, multi-aperture photometry and some preliminary mapping of the brighter sources in RCW 38, G291.6−0.5, G337.9−0.5, G333.6−0.2, H2–3, and RCW 97 do not show color changes much greater than 10 percent. In the case of RCW 57, the measured flux includes a contribution from RCW 57/IRS 1, an unresolved source which has deep absorption at 10 μ (FP). The contribution from IRS 1 to the flux measured with a 15″ aperture centered on IRS 2, the 10 μ peak, is about 15 percent. Such unresolved sources could affect the estimates of $\tau(9.8\ \mu)$ discussed below.

III. THE ABSORPTION AT 10 μ

In order to derive $\tau(9.8\ \mu)$ from the data, some simple models for the 10 μ energy distributions were constructed. These models are completely analogous to those of Gillett *et al.* (1975). The underlying emission is assumed to arise from dust particles heated to a uniform temperature T by an unspecified source. They radiate their energy according to an emission law of the form $Q(a, \lambda)B_\lambda(T)$, where Q is the emissivity for particles of size a, and B_λ is the blackbody function. The emission from an ensemble of such particles is proportional to $B_\lambda(T)\{1 - \exp[-\alpha Q(a, \lambda)]\}$, where $\alpha Q(a, \lambda)$ is the emission optical depth through the nebula. A surrounding cloud of particles, much cooler than those which are emitting, and which have the same $Q(a, \lambda)$ function absorbs this radiation, and a fraction $\exp[-\tau(\lambda)] = \exp[-\beta Q(a, \lambda)]$ escapes. The three parameters, α, β, and T, and the form of $Q(a, \lambda)$ then specify a model. It is assumed that the emission is optically thin, since in two sources, the Trapezium and RCW 38, the silicate feature appears in emission. Since only the colors are of interest, the parameter α can

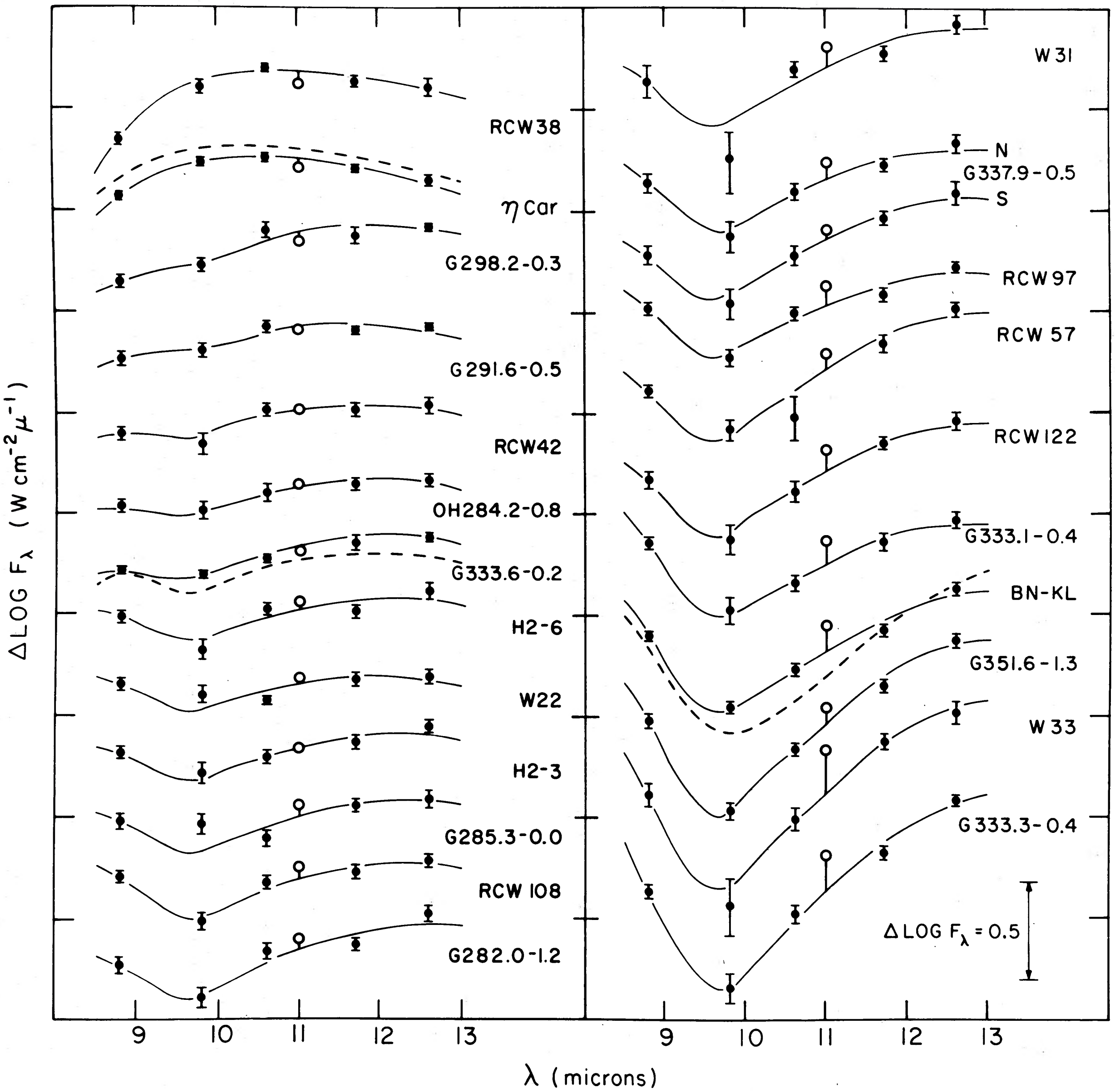

FIG. 1.—Energy distributions of H II regions. *Closed circles*, observed points (on arbitrary flux scales) and 1 σ_m errors. *Open circles*, broad-band 10 μ observations. *Thin solid lines*, the best fitting models; *dashed lines*, published high-resolution spectra. The observations of BN were made with a 22″ aperture and 45″ east-west beam separation. The observations by Gillett and Forrest (1973) were made with an 11″ aperture and a 15″ beam separation. The fit for BN (and the value of $\tau(9.8\ \mu)$ plotted in Fig. 2) was found by assuming an underlying blackbody spectrum. The dashed curve for G333.6−0.2 has been displaced upward by 0.1 for convenience.

be set equal to any number $\ll 1$ (0.01 was chosen for all sources).

As a check on the assumption of small optical depth in the underlying emission at 10 μ, one can compare the brightness temperatures T_b (corrected for silicate absorption) and color temperatures T_c, found either from Table 1 or from the 10 μ/20 μ colors (see FP). In all cases $T_b < T_c$, and hence if silicate particles are responsible for the underlying spectrum, then choosing $\alpha \ll 1$ is reasonable. The function $Q(a, \lambda)$ is the same as that used by Gillett *et al.* (1975) and is normalized to unity at 9.8 μ. The shape is derived directly from the Trapezium emission spectrum and depends only on the assumption that the temperature of the emitting dust is near 250 K. Thus, the analysis is on a firm observational basis, and rests on the suppositions that all of the underlying spectra are optically thin and that $Q(a, \lambda)$ is similar for all sources.

Spectra were predicted for a range of T and β, and the best fit to the data, in a least-squares sense, was found for each object. In calculating these fits, the error-weighted mean flux was used for normalization. This eliminates possible error caused by normalizing to only one wavelength. The finite widths of the filters were compensated for by first finding approximate τ and T values, convolving the known filter responses with the predicted spectrum, and then adding a correction to the observed fluxes to convert them to "monochromatic" fluxes. This adjustment is largest for the sources with deep absorption, but in no case exceeds 0.05 mag. Values for τ and T were then recalculated and are listed in Table 1. The solid curves in Figure 1 are the final predicted spectra. The intermediate-band points have been plotted as adjusted for filter response.

The agreement between the data points and the predicted spectra and the values of the reduced χ squares $\chi^2_R = \chi^2/(N-3)$ listed in Table 1 show that the fits are satisfactory. These values of χ^2_R are formal, since they do not take into account the fact that the filters are not all linearly independent. This is especially true of the 11.7 μ filter which overlaps the two adjacent ones. Thus the values of χ^2_R should probably increase by about 50 percent. The mean 1 σ_m uncertainty in $\tau(9.8\ \mu)$ is found to be $\sigma_\tau = 0.15 + 0.07\,\chi^2_R$. These uncertainties show that the important quantity, $\tau(9.8\ \mu)$, can be adequately determined using five intermediate-band filters.[1] We conclude, therefore, that the 8–13 μ energy distributions of the infrared sources associated with H II regions presented in this paper can be adequately accounted for by a combination of emission and absorption by silicate particles.

The only parameter which can affect the τ values significantly is α, if $\alpha > 1.0$. Changing α from 0.01 to 5.0 shifts all τ values downward by the constant 1.3. T is not important in determining the value of $\tau(9.8\ \mu)$, because the wavelength baseline is short. Similarly, the exact shape of $Q(a, \lambda)$ is not critical since to first order a change in $Q(a, \lambda)$ will change T rather than τ. In any event, the quality of the fits shows that the adopted shape of $Q(a, \lambda)$ is reasonable. In G333.6−0.2, the 12.8 μ Ne^+ line has been observed (Aitken and Jones 1974). If this line is present in the other objects, it will affect the 12.6 μ data point. For G333.6−0.2, the correction amounts to 0.11 mag and hence has a negligible effect on $\tau(9.8\ \mu)$.

Table 1 lists values of $\Delta \log F_\lambda(10\ \mu)$. These are the corrections to the observed broad-band 10 μ fluxes, which are due to the silicate absorption feature. A second conclusion of this paper (also pointed out by Gillett *et al.* 1975) is that these corrections are quite substantial, and can amount to as much as a factor of 20. Since the silicates also have a spectral feature in the 20 μ window (although $\tau[20\ \mu]$ is probably less than $\tau[10\ \mu]$), in every case the broad-band 10–20 μ color temperatures and the 1–25 μ luminosities will increase, the latter by as much as a factor of 5. The implications of these points for the energetics of the infrared sources will be discussed in a later paper.

IV. OTHER ABSORPTION FEATURES

Table 1 lists values of three absorption indicators. The values of $\tau(H_2CO)$ were computed from T_L/T_C values given by Whiteoak and Gardner (1974). In each case, the formaldehyde component which has a velocity close to that of the nebular H109α line was used. Thus the H_2CO clouds are expected to be circumnebular rather than interstellar. The values of A_V were found from the observed $[1.65\ \mu] - [2.2\ \mu]$ colors, and by assuming that the emission at these wavelengths is hydrogenic recombination. The data are either taken from FP or are unpublished. The parameter $\tau(3.1\ \mu)$ measures the ice-band absorption at 3.1 μ—these values were found using new data (to be published). Briefly, a continuum is defined by the broad-band 2.2 and 3.5 μ measurements, and the absorption is measured with a filter at $\lambda_0 = 3.10$ ($\Delta\lambda = 0.08$).

Figure 2 shows the relationship of $\tau(9.8\ \mu)$ to these indices. There is no apparent correlation of $\tau(9.8\ \mu)$ with A_V, although this conclusion is weak because of a lack of sufficient data points, the assumption of pure recombination emission, and the probable existence of nonuniform reddening. Our estimates of $\tau(3.1\ \mu)$ can be seriously affected by the presence of a broad emission feature at 3.3 μ, which has been seen in some H II regions (Gillett and Grasdalen 1975). Thus, the values of $\tau(3.1\ \mu)$ presented here should be regarded as upper limits to the true ice absorption. Nevertheless, the limited data available point to a sharp distinction between those infrared sources most likely associated with H II regions and BN and OH 284.2−0.8. Clearly, higher resolution spectral scans are needed to further investigate the ice feature.

The correlation of $\tau(9.8\ \mu)$ with formaldehyde optical depth (Fig. 2) is unambiguous and agrees with the preliminary results noted in FP: $\tau(9.8\ \mu)$ increases with $\tau(H_2CO)$, and must exceed 2 in order that $\tau(H_2CO)$ exceed 0.03. The plot of $\tau(9.8\ \mu)$ against log (H_2CO column density) also shows a distinct correlation. The column densities were calculated according to the precepts of Gardner, Dickel, and Whiteoak (1973) and by assuming that the transition temperature of the levels in H_2CO is 1.7 K for all sources. Thus, absorption caused by silicates and H_2CO are related, though in a nonlinear way. Since the H_2CO extinction originates in the circumnebular molecular clouds, it follows that the bulk of the silicate extinction must arise from these same clouds.

A schematic interpretation of Figure 2 is the following: the H_2CO formation process depends sensitively on the density of H_2 (Dalgarno, Oppenheimer, and Black 1973). Since H_2 probably forms on grain surfaces, the H_2 density will be sensitive both to

[1] $\tau(9.8\ \mu)$ can be estimated from a 10 μ (broad-band)/9.8 μ color. A plot of $\tau(9.8\ \mu)$ versus $\Delta \equiv \Delta \log [F_\lambda(10\ \mu)/F_\lambda(9.8\ \mu)]$ has a correlation coefficient of 0.94 and gives

$$\tau = (0.84 \pm 0.02) + (8.1 \pm 0.6)\Delta\ .$$

Since complete data for RCW 110B were not obtained, its value of $\tau(9.8\ \mu)$ in Table 1 is that found from this relationship.

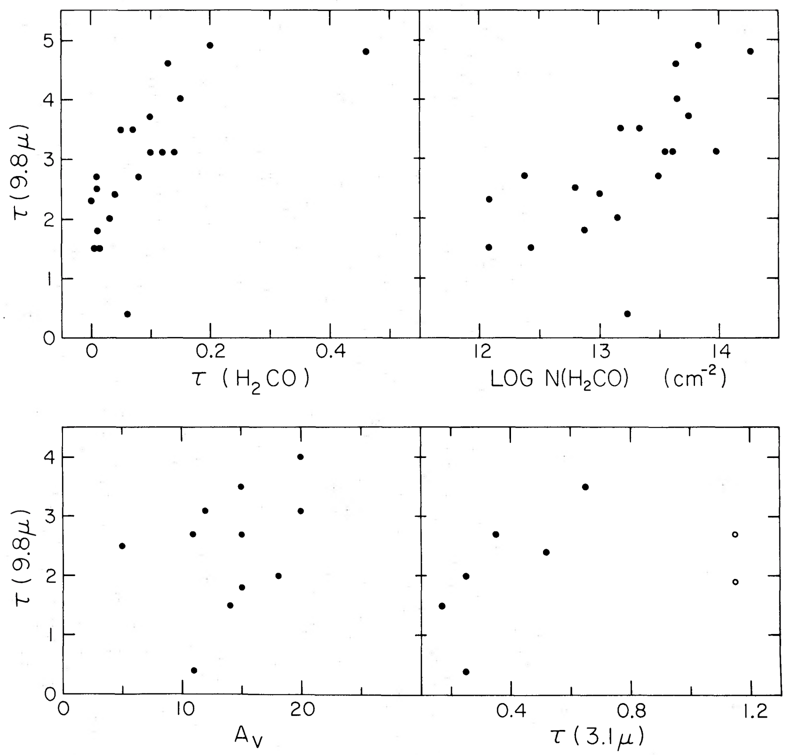

FIG. 2.—Plots of silicate extinction, $\tau(9.8\ \mu)$, against other measures of extinction toward H II regions. In the $\tau(3.1\ \mu)$ plot, the upper open circle is BN and the lower is OH 284.2−0.8. The errors in the values of A_v are ±5 mag.

gas density and grain density. Furthermore, the photodissociation rates of both molecules depend on the attenuation of UV radiation by grains. Thus, the density of H_2CO molecules is expected to be a very sensitive function of grain density. If $\tau(9.8\ \mu)$ can be considered to give some measure of the amount of absorbing material along the line of sight to an H II region or protostar, then the sensitivity of the H_2CO formation and destruction rates to grain density and extinction leads to the conclusion that beyond some value of $\tau(9.8\ \mu)$ the increase in $\tau(H_2CO)$ or H_2CO column density should be rapid.

An effect which could influence the interpretation of Figure 2 would be the presence of H_2CO emission as found by Downes and Wilson (1974) toward NGC 7538. Also, the difference in beam size used for the radio and infrared measurements may be important if subsequent observations show $\tau(9.8\ \mu)$ to vary substantially from point to point. This latter effect is reduced, however, since the value of $\tau(H_2CO)$ measured will be most strongly weighted toward that part of the source which has the brightest continuum background, and this corresponds to the region measured in the infrared. Furthermore, recent measurements of H_2CO absorption in the direction of a rather complex infrared H II region (W3) by Whiteoak, Rogstad, and Lockhart (1974) with 20″ resolution showed no significant spatial variations in optical depth. Despite the above qualifications, the correlation between $\tau(H_2CO)$ and $\tau(9.8\ \mu)$ exists and appears to be secure.

V. SUMMARY AND CONCLUSIONS

1. Five intermediate bandwidth filters can be used to determine the shape of the 8–13 μ silicate feature in galactic H II regions to reasonable accuracy.

2. A simple two-parameter model fits all of the energy distributions adequately and gives reasonable estimates of the silicate optical depth $\tau(9.8\ \mu)$. The values of $\tau(9.8\ \mu)$ range from 0.4 to 5 in our sample of sources.

3. The extinction in the 10 μ window can be substantial (as much as a factor of 20). The implied corrections to the 1–25 μ luminosities of these objects can be as great as a factor of 5, depending on the value of $\tau(9.8\ \mu)$ and the behavior of $Q(a, \lambda)$ in the 20 μ region.

4. The values of $\tau(9.8\ \mu)$ are related in a direct but nonlinear way to measures of the 6 cm H_2CO optical depths and column densities. As in FP, we interpret this relationship to mean that most of the silicate extinction arises in the circumnebular clouds rather than the intervening interstellar medium.

5. So far, not enough data exist to demonstrate any correlation (or lack thereof) of $\tau(9.8\ \mu)$ with other measures of the extinction toward the H II regions.

Note added 1976 May 10.—Estimates of A_v have been determined from recent measurements of $[1.65\ \mu] - [2.2\ \mu]$ colors of four objects in Table 1. The objects and A_v (mag) values are: G333.1−0.4, 8; G282.0−1.2, 11; G348.2−1.0, 9; G348.7−1.0, 17. The addition of these points does not alter the character of Figure 2—$\tau(9.8\ \mu)$ versus A_v.

REFERENCES

Aitken, D. K., and Jones, B. 1973, *Ap. J.*, **184**, 127.
———. 1974, *M.N.R.A.S.*, **167**, 11P.
Becklin, E. E., Frogel, J. A., Kleinmann, D. E., Neugebauer, G., Persson, S. E., and Wynn-Williams, C. G. 1974, *Ap. J.*, **187**, 487.
Becklin, E. E., Frogel, J. A., Neugebauer, G., Persson, S. E., and Wynn-Williams, C. G. 1973, *Ap. J.* (*Letters*), **182**, L125.
Dalgarno, A., Oppenheimer, M., and Black, J. H. 1973, *Nature Phys. Sci.*, **245**, 100.
Downes, D., and Wilson, T. L. 1974, *Ap. J.* (*Letters*), **191**, L77.
Frogel, J. A., and Persson, S. E. 1974, *Ap. J.*, **192**, 351 (FP).
———. 1975, *ibid.*, **197**, 351.
Frogel, J. A., Persson, S. E., and Aaronson, M. 1976, in preparation.
Gardner, F. F., Dickel, H., and Whiteoak, J. B. 1973, *Astr. and Ap.*, **23**, 51.
Gehrz, R. D., Hackwell, J. A., and Smith, J. R. 1975, *Ap. J.* (*Letters*), **202**, L33.
Gillett, F. C., and Forrest, W. J. 1973, *Ap. J.*, **179**, 483.
Gillett, F. C., Forrest, W. J., Merrill, K. M., Capps, R. W., and Soifer, B. T. 1975, *Ap. J.*, **200**, 609.
Gillett, F. C., and Grasdalen, G. L. 1975, private communication.
Merrill, K. M., and Soifer, B. T. 1974, *Ap. J.* (*Letters*), **189**, L27.
Stein, W. A., and Gillett, F. C. 1969, *Ap. J.* (*Letters*), **155**, L197.
Whiteoak, J. B., and Gardner, F. F 1974, *Astr. and Ap.*, **37**, 384.
Whiteoak, J. B., Rogstad, D. H., and Lockhart, I. A. 1974, *M.N.R.A.S.*, **169**, 59P.
Woolf, N. J. 1972, in *Proc. IAU Symposium 52, Interstellar Dust and Related Topics*, ed. J. M. Greenberg and H. C. van de Hulst (Boston: Reidel).

Marc Aaronson: Center for Astrophysics, 60 Garden Street, Cambridge, MA 02138

Jay A. Frogel: Kitt Peak National Observatory, P.O. Box 26732, Tucson, AZ 85726

S. Eric Persson: Hale Observatories, 813 Santa Barbara Street, Pasadena, CA 91101